Raman and photoluminescence analysis of stress state and impurity distribution in diamond thin films

Cite as: Journal of Applied Physics **78**, 6709 (1995); https://doi.org/10.1063/1.360495
Submitted: 16 June 1995 • Accepted: 16 August 1995 • Published Online: 17 August 1998

L. Bergman and R. J. Nemanich

Raman and photoluminescence analysis of stress state and impurity distribution in diamond thin films

L. Bergman and R. J. Nemanich[a)]
Department of Physics and Department of Materials Science and Engineering, North Carolina State University, Raleigh, North Carolina 27695-8202

(Received 16 June 1995; accepted for publication 16 August 1995)

Photoluminescence (PL) and Raman spectroscopy were employed to investigate the nature and sources of stress and the type and distribution of impurities and defects in thin diamond films grown on silicon substrates. The types of impurities and defects which were detected in the diamond films are the nitrogen, silicon, and the sp^2-type bonding of the graphitic phase. Our Raman analyses indicate that the diamond films exhibit a net compressive stress. After compensating for the thermal interfacial stress and for the stress due to grain boundaries it was found that the residual internal stress is compressive in nature. From Raman line-shape analysis it was determined that the internal stress is due to the various impurities and defects present in the film. Moreover, the stress magnitude exhibits a strong correlation with the graphitic phase implying that the sp^2 bonding produces a dominant compressive stress field. The PL analytical line-shape investigation of the nitrogen band at 2.154 eV indicates that the nitrogen centers are uniformly distributed in the film. The PL line shape exhibited a close fit to the Lorentzian–Gaussian convoluted line known as the Voit profile. The deconvolution of the line resulted in a dominant Gaussian component, corresponding to stress arising from line type defects, and a much smaller Lorentzian component corresponding to point defect stress. The Gaussian component was attributed to the graphitic phase implying that the sp^2 bonding is not in the form of a point defect but rather takes the form of a line or extended defect. The line-shape investigation of the silicon band at 1.681 eV showed that the silicon centers are correlated with the silicon/diamond interfacial stress. Finally, the response of the nitrogen and silicon optical centers to the internal stress, which is manifested via the PL linewidth, was also studied. The silicon band exhibits the narrower linewidth which may indicate that the silicon center complies less to the internal stress than the nitrogen center or that the two optical centers are interacting with different types of stress sources. © *1995 American Institute of Physics.*

I. INTRODUCTION

Knowledge about the origins and characteristics of internal stress in diamond films is critical to advances in film quality since stress may interfere with and degrade the mechanical as well as the transport and optical properties of the films. Raman and photoluminescence (PL) spectroscopy have proven to be useful and nondestructive techniques for evaluating the stress of crystals and films.[1–13] In this research we extend these techniques to the analysis of stress in diamond thin films with different impurity concentrations arising from different growth conditions, and show that the impurities and defects are the main source of the internal stress.

The first part of our investigation focuses on Raman analysis of the nature and sources of stress in diamond films. It has previously been determined that the Raman line frequency shifts linearly with stress; by applying this correlation to observed line frequency shift, information about the stress type (i.e., compressive or tensile) and stress magnitude may be obtained.[1,2] Our Raman analysis of the peak positions indicated that all of the diamond films studied exhibit a net compressive stress ranging from 0.37 to 2.21 GPa. The net compressive stress for each film, as determined from the Raman line shift, was then separated into the compressive and tensile components. The stress deconvolution was based on previous models for applicable stress sources in diamond films such as the compressive interfacial thermal stress[14,15] and the tensile stress imposed by grain boundaries,[15,16] and is discussed in detail in Sec. III. After compensating for these stresses, it was determined that the diamond films still exhibited residual internal compressive stress on the order of 0.25–2.02 GPa.

In order to assign a source to the internal compressive stress of the films, a Raman line-shape study was carried out as well as an investigation of the correlation of the internal stress to the Raman linewidth and impurity concentration. The Raman linewidth in general can be broadened via several mechanisms: The main mechanisms applicable to the diamond line are homogeneous broadening[17] and broadening due to size effect of the crystal.[18,20] Homogeneous broadening arises from a decrease of the lifetime of the crystal phonons. The theory of homogeneous spectral line shape predicts that the linewidth is inversely proportional to the phonon lifetime and that the line shape is expected to be a Lorentzian.[21] The other possible mechanism which results in Raman line broadening is phonon confinement in a small domain size.[18] The model developed to explain this mechanism is based on the uncertainty principle, which states that the smaller the domain size, the larger the range of different phonons that are allowed to participate in the Raman process. According to this model, as the linewidth gets broader

a)Electronic mail: robert_nemanich@ncsu.edu

 0021-8979/95/78(11)/6709/11/$6.00

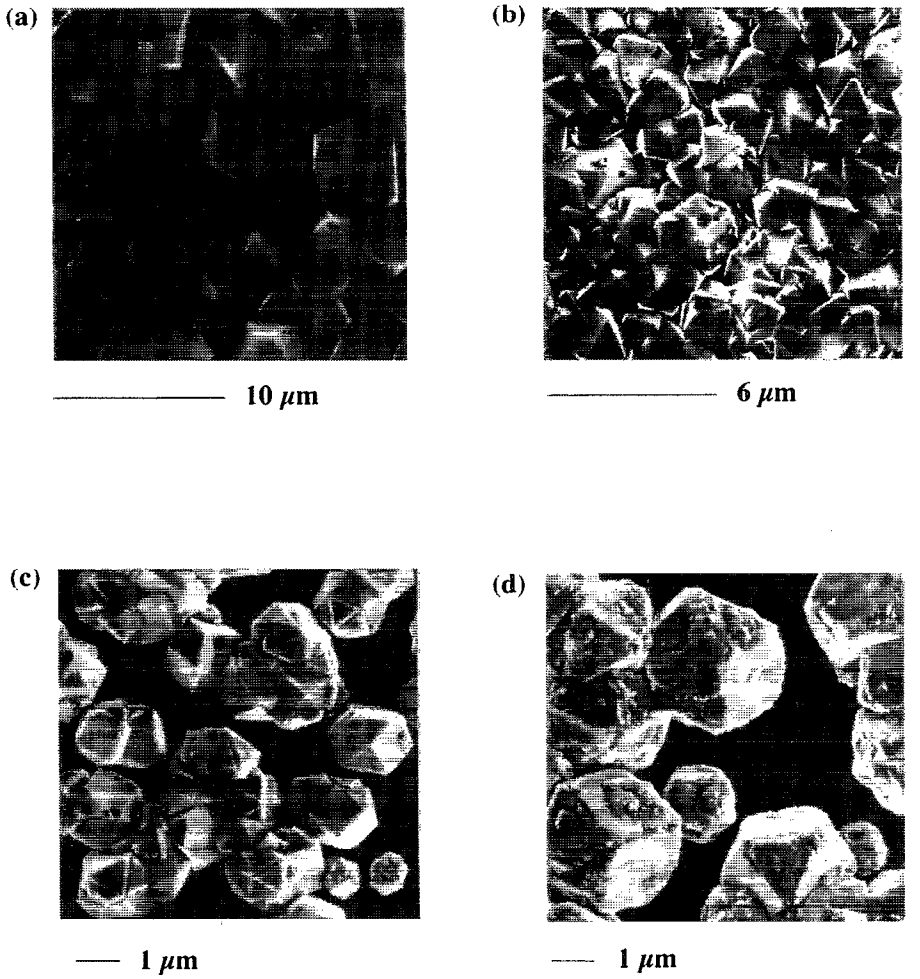

FIG. 1. The SEM micrographs of the (a) combustion, (b) 20 h, (c) HF 0%N, and (d) the HF 0.2%N diamond film.

the Raman peak shifts to a lower frequency and the line shape becomes asymmetric.

Our analysis indicates that the Raman linewidth is directly correlated with the internal compressive stress and that the Raman line shape exhibits a symmetric Lorentzian profile. These findings suggest that the dominant source is one which acts to shorten the phonon lifetime and at the same time induces internal compressive stress. Moreover, the internal stress exhibits a correlation with the graphitic phase (sp^2) concentration; a small deviation from linearity was consistent with the relative concentration of the other impurities present in the films. The above results lead us to conclude that the source of internal compressive stress in the diamond thin films are the various impurities and defects, and that the sp^2-type bonding is, with high likelihood, the principal stress source.

In the second part of our investigation the stress state of the diamond films is analyzed utilizing PL spectroscopy. Through the PL line-shape analysis additional knowledge was gained about the impurity and defect strain sources as well as their distribution in the film. The PL stress results were also compared to those found from the Raman analysis to show consistency between the PL and the Raman techniques. Our investigations focused on PL line-shape analysis of the 2.154 eV nitrogen-vacancy optical band and the 1.681 eV silicon band.[22–33]

In diamond crystal at low temperatures the PL line shape is determined almost entirely by the crystal strain inhomogeneities. The inhomogeneous broadening is at least 1000 times greater than the homogeneous broadening,[11] the latter of which arises from the lifetime characteristics of a transition. In general, the principal mechanism of the inhomogeneous broadening at low temperatures is the strain broadening that arises from the presence of dislocation-type defects and point defects in the crystal.[9–12] The defects introduce strain fields throughout the crystal that interact with and perturb the optical transitions energies. The statistical distribution and density of the optical centers and defects in the crystal as well as defect type determine the variations in the transition energies of the optical centers and the respective PL line shape.

To determine the stress sources and distributions we applied the well-established theoretical work developed by Stoneham on the strain broadening mechanisms of spectral bands.[9,10] In the following paragraph a brief summary of Stoneham's relevant results is presented.[9]

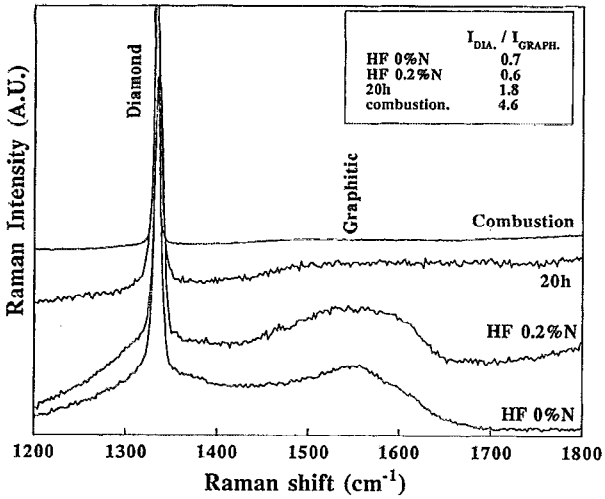

FIG. 2. The Raman spectra of the four diamond films, showing the diamond and the graphitic signals.

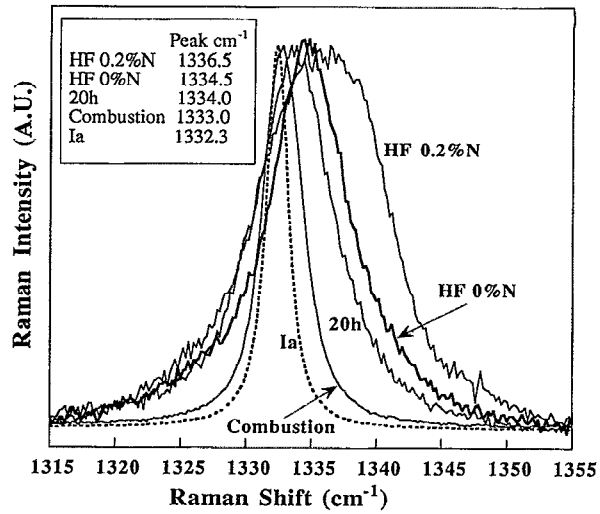

FIG. 3. The normalized high-resolution Raman spectra of the diamond signal of the films. The spectra of Ia crystal diamond is also included as a reference line.

(a) For a symmetric lattice, in which the lattice sites accommodate at random the optical centers and defects, the line shape is expected to be symmetric.

(b) When the strain in the crystal arises solely from uniformly distributed point defects the luminescence line shape is expected to be a Lorentzian.

(c) When the sources of the strain in the crystal are uniformly distributed dislocations (line-type defects) the line shape is expected to be a Gaussian.

(d) In the case when both types of defects are present in the crystal, the resulting line is the convoluted line shape of the Gaussian and the Lorentzian: This line shape is known as the Voit profile and has no closed-form mathematical expression. The relative linewidths of the Gaussian component and the Lorentzian component in the Voit profile reflect which defect is the dominant stress source in the crystal. The above results of Stoneham assumed an ideal continuous single crystal for which the spatial distribution of the defects and the optical centers were taken to be uniform.

The diamond films studied here contain a variety of defect types whose relative contribution to the stress should be determined. In addition to the silicon and nitrogen impurity point-type defects, a high concentration of line defects of dislocation type have been found in diamond films similar to ours utilizing transmission electron microscopy (TEM) spectroscopy.[34–36] Furthermore, the graphitic phase, which is the most common defect in diamond films,[37–39] has not yet been definitely classified as to being a point- or a line-type defect; hence, an optical analysis similar to that proposed by Stoneham may be useful in order to classify the graphitic phase and to differentiate the relative contributions of the other defect types to the strain. Moreover, due to the substrate interface the diamond films are not in the category of the ideal crystals assumed in Stoneham's work and we expect some of the PL line shape to be influenced by the deviation from the ideal. Therefore, an investigation of the PL line shape might also give insight into the effect of the substrate on the optical properties of the films.

PL line-shape investigations were undertaken for both the 2.154 eV nitrogen-vacancy optical band and the silicon band at 1.681 eV. It was found that the 2.154 eV PL line shape is symmetric and constitutes a Voit profile. The deconvolution of the line resulted in a dominant Gaussian component, corresponding to stress arising from line-type defects, and a much smaller Lorentzian component corresponding to point defect stress. The internal stress magnitude which was inferred from the PL linewidth is consistent with the one obtained from the Raman analysis. The above results suggest that the nitrogen PL centers and the interacting defects are uniformly distributed throughout the film and that the dominant defect which acts as a stress source is not in the form of a point defect. Furthermore, the Lorentzian linewidth was found to be consistent with and thus completely accounted for by the total nitrogen concentration (which is known to be a point defect) which left the only feasible assignment of the dominant Gaussian component (besides that portion assigned to the dislocation) to the graphitic phase. This implies that the sp^2 bonding is in the form of a line or extended defect.

The preliminary results of PL line-shape analysis of the silicon center at 1.681 eV show that the PL line exhibits a strong asymmetry. The line-shape investigation excluded the possibility that the line asymmetry arises from an underlying PL band due to a different optical center which luminesces in the same energy range. In our previous work it was concluded that the silicon centers reside mainly next to the silicon–diamond interface.[32] Therefore we tentatively attribute the line asymmetry to some form of interfacial stress interaction. Furthermore, it was observed that the 1.681 eV linewidth is narrower than the linewidth of the nitrogen PL band at 2.154. In general a comparison of different PL linewidths (arising from different optical centers residing in the same crystal) might convey information about the structure of the centers as well as the stress environment.[9,22] We propose two possibly simultaneously acting mechanisms to explain the difference in the linewidths:

TABLE I. The Raman characteristics of the diamond films and the experimental stress values as calculated from the Raman shift $\Delta\nu$.

Film	$I_{\text{graphitic}}/I_{\text{diamond}}$	FWHM (cm^{-1})	Peak (cm^{-1})	$\Delta\nu$ (cm^{-1})	σ_{expt} (GPa)
Combustion	0.22	3.6	1333.0	0.7	−0.37
20 h	0.55	6.8	1334.0	1.7	−0.90
HF 0%N	1.43	7.5	1334.5	2.2	−1.16
HF 0.2%N	1.67	11.7	1336.5	4.2	−2.21

(a) The silicon center is a more rigid center than the nitrogen center and hence does not comply to the stress as much as does the nitrogen center, and
(b) the stress acting upon the silicon centers and the nitrogen centers are of different origins.

The remainder of this article is organized as follows. Section II presents the experimental setup. In Sec. III Raman analysis of the stress in four diamond films is presented. Section IV presents the PL line-shape analysis of the films.

II. EXPERIMENT

Four diamond samples were involved in the research presented here and are referred to as the 20 h, HF 0%N, HF 0.2%N, and the combustion sample. Figure 1 shows scanning electron microscopy (SEM) micrographs of the surfaces of the samples. The 20 h sample was grown utilizing the microwave chemical-vapor-deposition (CVD) method; the plasma consisted of 1% CH_4 in H_2 at 1000 sccm total flow. The plasma power, pressure, and substrate temperature were maintained at 800 W, 25 Torr, and 750 °C, respectively. The growth time for the 20 h sample was 20 h and the film was ~2 μm thick and of a continuous morphology. The HF 0%N and the HF 0.2%N were prepared utilizing the hot filament growth method. (The %N in the sample names reflects the percentage of N_2/H_2 in the gas phase). The growth time was 6 h and the growth temperature was 850 °C. The plasma consisted of 1.5% CH_4 in H_2 and the filament temperature was maintained at 2000 °C. The combustion sample was grown for 0.5 h in a controlled combustion chamber.[40] The growth temperature was 1000 °C and the film was ~3 μm thick. All the samples were grown on (100)-oriented silicon substrates.

The Raman spectra were obtained via the micro mode at room temperature employing the argon-ion laser 514.53 nm excitation line which was focused on the sample to a spot size ~5 μm in diameter. The low-temperature PL spectra were acquired at 10 K via the macro mode employing the 514.53 nm laser line which was focused on the sample to a spot size ~2 mm×100 μm. The experimental conditions, for the high-resolution Raman and PL data acquisition, were set to allow the spectral resolution to be 1 and 2 cm^{-1}, respectively.

III. RAMAN ANALYSIS

A. Stress calculation

In this subsection a Raman analysis of the stress of the diamond thin films is presented. Figure 2 shows the diamond and the graphitic Raman signals of the four samples; Fig. 3 shows the high-resolution normalized Raman spectra of the diamond signal of the samples as well as the spectra obtained from Ia crystal diamond. It can be seen in Fig. 3 that the Raman peak position of the four diamonds exhibits a shift to a higher frequency relative to the peak of the Ia diamond.

It has been shown that upon applying compressive stress on the diamond, the peak position of the Raman line shifts linearly with the stress to a higher frequency.[1] The dependence of the Raman shift $\Delta\nu$ on the applied stress σ is

$$\Delta\nu = \nu - \nu_0 = -\alpha\sigma, \tag{1}$$

where α is the pressure coefficient[1,2,8] and ν_0 is taken to be the Raman peak position of the natural diamond when no pressure is applied. The peak position ν_0 of natural and synthetic diamond crystals at room temperature has been reported to be in the range 1332.1–1332.6 cm^{-1} with a full width at half-maximum (FWHM) in the order of 1.8 cm^{-1}.[17] The above published results are in agreement with our observations of the Raman peak position at 1332.3±0.2 cm^{-1} and linewidth ~2 cm^{-1} of a type-Ia diamond crystal. In order to estimate the experimental stress in the diamond samples σ_{expt} Eq. (1) is used with $\nu_0 = 1332.3$ cm^{-1} and with an average value of the pressure coefficient $\alpha = 1.9$ cm^{-1}/GPa. The results of the calculations are listed in Table I as well as the Raman characteristics obtained from Figs. 2 and 3. The above calculations clearly indicate that all of the diamond films involved in this study exhibit a net compressive (negative) stress. Furthermore, the combustion film was found to exhibit the lowest compressive stress while the HF 0.2%N exhibited the greatest compressive stress.

Next we analyze the sources of stress in the diamond films by identifying the stress components and estimating the contributions to the net stress σ_{expt} in each of the diamond samples. The contributions to the net stress may be either tensile or compressive. The observable net stress σ_{net} in the diamond films is given by Eq. (2) in terms of the thermal stress σ_{TH}, the sum of the internal stresses $\Sigma\sigma_{\text{IN}}$, and the stress due to silicon–diamond lattice mismatch σ_{lm},[41]

$$\sigma_{\text{net}} = \sigma_{\text{TH}} + \Sigma\sigma_{\text{IN}} + \sigma_{\text{lm}}. \tag{2}$$

The thermal stress σ_{TH} arises from the difference in the thermal-expansion coefficients of silicon and diamond.[14,15] As a result of this difference, the silicon substrate contracts more than the diamond film upon cooling from the elevated growth temperature down to room temperature. Hence, the silicon substrate applies compressive stress on the diamond film.The dependence of the thermal stress on the deposition temperature has been previously calculated by Wind-

TABLE II. The experimental and the calculated stress components of the diamond films.

Sample	σ_{expt} (GPa)	σ_{TH} (GPa)	σ_{GB} (GPa)	$\sigma_{calc}=\sigma_{TH}+\sigma_{GB}$	Δ (GPa) $=\sigma_{expt}-\sigma_{calc}$
Combustion	−0.37	−0.155	+0.03	−0.125	−0.25
20 h	−0.90	−0.25	+0.104	−0.146	−0.75
HF 0%N	−1.16	−0.23	+0.07	−0.16	−1.00
HF 0.2%N	−2.21	−0.23	+0.042	−0.188	−2.02

ischmann *et al.*[15] Using the results of Ref. 15, we anticipate that the 20 h sample (750 °C) should have a compressive thermal stress component ~0.25 GPa, the two HF samples (850 °C) should exhibit a lower stress ~0.23 GPa, and the combustion sample (1000 °C) should be under the lowest thermal stress ~0.15 GPa.

The total internal stress component $\Sigma\sigma_{IN}$ in the diamond film may be due to various sources such as impurities, structural extended defects such as dislocations, and interactions across grain boundaries. The interactions across grain boundaries has been reported to be the possible origin of the main intrinsic tensile stress σ_{GB} in the diamond films.[15,42] According to the model developed by Doljack and Hoffman,[16] when the grains start to coalesce, they exert attractive forces across the boundaries. This relaxation mechanism is energetically favored by the system since the grain boundary interfacial energy is less than the energy of the two separated grain surfaces. The relaxation mechanism, however, is constrained by the adhesion of the grains to the substrate which causes an internal tensile stress to be present in the film. The intrinsic tensile stress σ_{GB} has been found to be inversely proportional to the average grain diameter d in a sample,

$$\sigma_{GB}=[E(1-\nu)](\delta/d), \tag{3}$$

where $\delta=0.077$ nm is the constrained relaxation lattice constant of diamond and $E(1-\nu)=1345$ GPa is the mechanical constant of diamond.[15] The average grain size for the combustion, 20 h, HF 0%N, and HF 0.2%N sample, as estimated from the SEM micrographs, is ~3.5, 1, 1.5, and 2.5 μm, respectively. The values of σ_{GB} as well as the values of the other stress components are listed in Table II.

The other term in Eq. (2) to be discussed next is the stress due to lattice mismatch σ_{lm}. The stress in the diamond due to its ~35% lattice mismatch with the silicon substrate or ~20% mismatch with the SiC buffer layer is expected to be tensile and for pseudomorphic growth to cause a very large Raman shift ~200 cm^{-1};[43] however, this order of magnitude shift was never observed in our diamond Raman lines. The absence of the large lattice-mismatch stress can be attributed mainly to the dislocation and to the grain misorientation relaxation mechanisms: A tilt of about 35° (an expected value in our high-angle boundary polycrystalline films) may relax completely the interfacial stress existing between SiC and diamond.[44] Hence, we can safely ignore the effect of σ_{lm}.

From the results listed in Table II it may be concluded that the thermal stress and the stress due to the grain-boundary interactions are not very significant, and that, after compensating for their contributions (σ_{calc}), the samples still exhibit an appreciable excess of compressive stress which we refer to as delta (Δ). We suggest that the most probable origins of Δ are the various types of impurities and defects present in the diamond thin films. In the following subsection we present an investigation of this hypothesis.

B. Impurities and defects as intrinsic stress sources

Validation of the hypothesis that the intrinsic stress is due to defects and impurities may be obtained from analyzing the correlation of the Raman line broadening to the stress Δ arising from defects. Figure 4(a) presents such a correlation obtained from our samples; it can be seen that Δ is a linearly increasing function of the Raman broadening indicating that the origin of the Raman line broadening may be related to the internal stress in the diamond films. Since Raman line broadening can result from various mechanisms, as is discussed next, our objective is to differentiate among the mechanisms to find the origin of the dominant one and to determine its relation to the internal stress. One possible mechanism which results in broadening is the Raman pho-

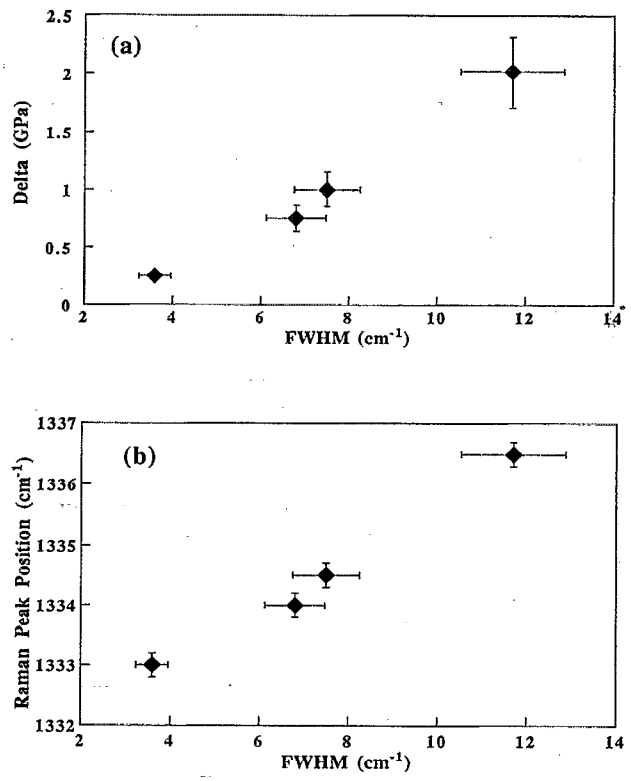

FIG. 4. The correlation between the Raman linewidth and (a) the internal compressive stress delta and (b) the Raman peak position.

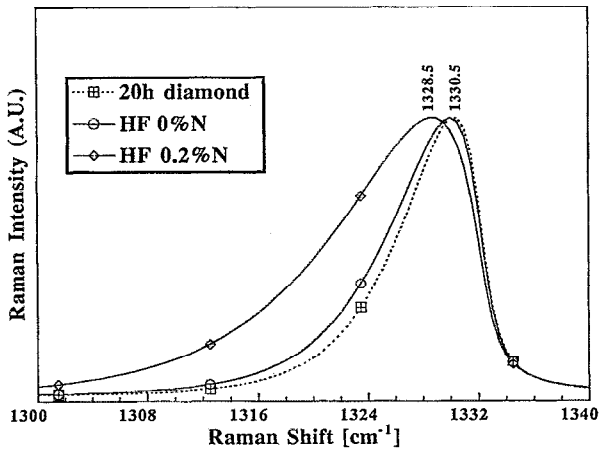

FIG. 5. The Raman diamond lineshape as calculated from Eq. (4) for the corresponding experimental widths of the 20 h, HF 0%N, and HF 0.2%N Raman signals.

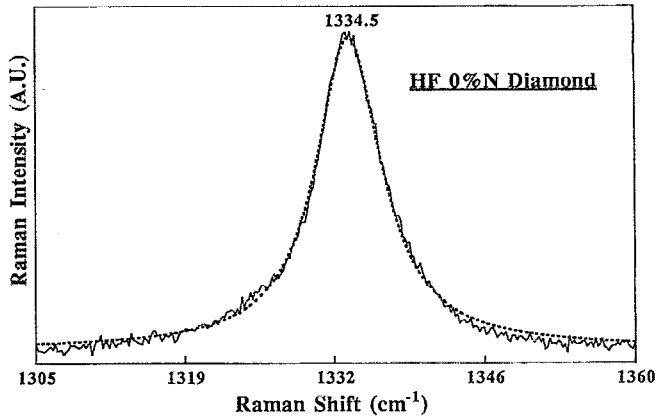

FIG. 6. A typical Raman line shape of the diamond films. The dashed line is the Lorentzian fit to the experimental line.

non confinement in a small domain size.[18–20] The well-established confinement model is based on the uncertainty principle, which states that the smaller the domain size, the larger the range of different phonons (with different q vector and different energy) that are allowed to participate in the Raman process. Hence, the broadening of the Raman line in this case is due to the spread in phonon energy. The Raman line shape in the phonon-confinement model is given by

$$I(w)\cong\int_0^1 \frac{dq\ \exp(-q^2L^2/4)4\pi q^2}{[\omega-\omega(q)]^2+(W_0/2)^2}, \tag{4}$$

where L is the confinement size, W_0 is the diamond natural linewidth ($\sim$2 cm^{-1}), and $\omega(q)$ is the phonon-dispersion curve of the form $A+B\cos(q\pi)$.[18–20] According to this model, as the width of the Raman line gets broader, the peak of the line shifts to a lower energy and the line shape becomes asymmetric. The correlation between the Raman linewidth and the peak position obtained from our diamonds is presented in Fig. 4(b). The data in the figure indicate that the peak positions shift to higher frequencies which is opposite in behavior to that predicted from the model. In order to examine the Raman line shape Eq. (4) was numerically evaluated to give the Raman line shape for L=86, 80, and 62 Å, which result in linewidths of 6.8, 7.5, and 11.7 cm^{-1}, respectively. These linewidths correspond to the 20 h, HF 0%N, and HF 0.2%N diamond linewidths. The expected Raman line shapes are shown in Fig. 5. As can be seen in the figure the confinement model predicts a large asymmetry in the Raman lineshape which was not observed in the Raman signal (see Figs. 3 and 6).

Symmetric Raman line shapes and correlation similar to ours have been reported by Ager and co-workers[20] who concluded that the broadening due to the confinement is not applicable when such a correlation is found. In light of the above we conclude that the domain size in our samples is sufficiently large so as to make the phonon confinement broadening negligible compared to other broadening mechanisms.

A more plausible mechanism for Raman broadening in diamond films has been suggested to be due to the phonon scattering (phonon decay) at impurities and defects.[20] The scattering event shortens the lifetime of the phonons and thus results in a broader Raman line. The Raman line shape due to the lifetime shortening is expected to be symmetric and of a Lorentzian line shape as was observed in our diamonds and which is depicted in Fig. 6. If the hypothesis that the defects are the source of the internal stress is correct, then the width of the Raman lines can be expected to correlate well with the defect stress Δ, as was indeed found in our work [see Fig. 4(a)]. The observed correlation between the Raman widths and Δ indicates that the various defects, which were argued to cause the broadening, are also the main cause of the compressive internal stress in the diamond films. Hence, we assign the origin of the excess compressive stress Δ to the various types of impurities and defects in the diamond film.

The identity of the types of impurities in the diamond films is inferred from the PL spectra presented in Fig. 7. It can be seen that the spectra of the HF 0.2%N sample exhibit the nitrogen-vacancy bands at 2.154 and 1.945 eV as well as their vibronic side bands. The silicon center band at 1.681 eV is very weak. The spectra of the HF 0%N sample does not show any of the nitrogen nor the silicon PL bands. The spectra of the 20 h diamond sample is dominated by the strong silicon band while the spectra of the combustion diamond exhibits the nitrogen as well as the silicon PL bands. In order to estimate the total concentration of the nitrogen impurity secondary-ion-mass spectroscopy (SIMS) has been utilized and it has been found that the HF 0.2%N and the combustion samples contain $\sim5\times10^{20}$ and 1×10^{20} N/cm^3, respectively (the other two films were found to contain nominal nitrogen concentration).

SIMS is not a very appropriate spectroscopy, however, for obtaining the total silicon impurity concentration in very thin films since an additional signal arises from the silicon substrate. Instead the relative amount of silicon in each of the diamond films was estimated from the total integrated area of the 1.681 eV PL band (when present in the spectra) relative to the diamond Raman integrated area. It was calculated that the ratio is $\sim$5 for the combustion and $\sim$50 for the 20 h

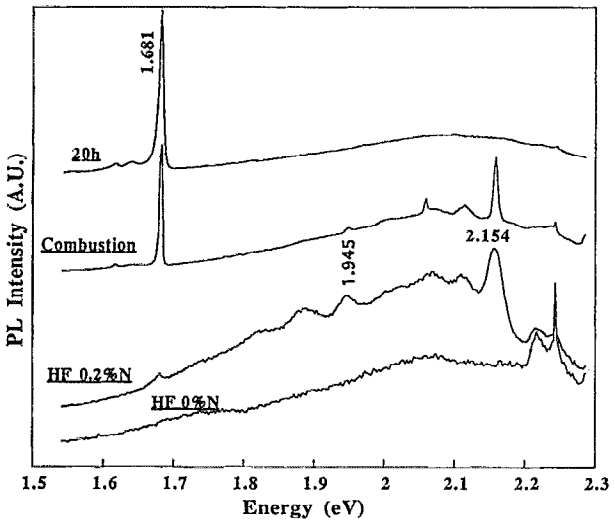

FIG. 7. The PL spectra of the diamond films. The nitrogen-related centers at 1.945 and 2.154 eV are present in the spectra of the combustion and the HF 0.2%N. The silicon center at 1.681 eV is present in the PL spectra of the combustion and the 20 h diamonds.

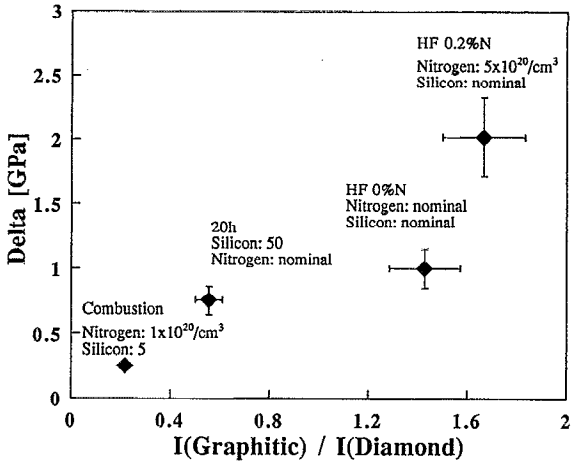

FIG. 8. The correlation between the internal stress Delta and the graphitic phase defect. Concentrations of the various impurities are also listed.

films, respectively. Another type of defect which is present in all the four films is the graphitic phase as can be seen from the Raman spectra in Fig. 2. The relative graphitic concentration $I_{\text{graphitic}}/I_{\text{diamond}}$ (obtained from the graphitic and diamond integrated areas of the Raman signals) as well as the previously found impurity concentrations are listed in Table III.

To investigate the role of the graphitic phase as a source of internal stress in our films, we plotted the relative quantity $I_{\text{graphitic}}/I_{\text{diamond}}$ versus the internal compressive stress Δ. The graph is shown in Fig. 8, and for each sample the other observed nongraphitic impurities are listed. The data presented in the figure suggest that the sp^2-type bonding induces a compressive stress field in the diamond matrix; the small deviation from linearity is consistent with the concentration of the nitrogen and silicon impurities (and with the probable contribution to the stress from extended type defects).

In the following section the stress state of our diamond films is analyzed utilizing PL spectroscopy. Through this PL line-shape analysis additional knowledge is gained about the impurity and defect strain sources as well as their distribution in the samples.

TABLE III. The impurity concentrations in the diamond films as obtained from Raman, PL, and SIMS spectroscopes.

Sample	$I_{\text{graphitic}}/I_{\text{diamond}}$ Raman integrated area	$I_{\text{silicon}}/I_{\text{diamond}}$ PL integrated area	Nitrogen (cm^{-3}) SIMS
Combustion	0.22	5	$\sim 1\times10^{20}$(0.06 at. %)
20 h	0.55	50	nominal
HF 0%N	1.43	nominal	nominal
HF 0.2%N	1.67	nominal	$\sim 5\times10^{20}$(0.28 at. %)

IV. PL LINE-SHAPE ANALYSIS AND STRESS ANALYSIS IN DIAMOND FILMS

A. The 2.154 eV nitrogen-vacancy optical center

In this subsection the 2.154 eV PL line-shape investigation is presented. The 2.154 eV PL line has been observed only in the spectra of the combustion film which contains $\sim 1\times10^{20}$ N/cm^3 (and a small relative concentration of Si), and in the spectra of the HF 0.2%N film which contains $\sim 5\times10^{20}$ N/cm^3 (and a nominal Si concentration).

The 2.154 eV nitrogen optical center was suggested in Refs. 13 and 45 to consist of one nitrogen atom and a vacancy (or vacancies). This center appears in nitrogen-free diamond crystals after nitrogen implantation and annealing, or in diamonds containing nitrogen (Ia,Ib) after radiation damage and annealing. The nitrogen atoms in diamond may appear in various configurations and forms (only some of which are optical centers); according to Davies[11,46,47] at least 95% of the total nitrogen atoms in type-I diamonds appear in the form of the small aggregate (which are considered as point defects) and this form has been established to be the main source of the strain.[11] One very common form of small aggregate consists of two nearest-neighbor nitrogen atoms which is referred to as the A aggregate. While the A aggregate is not PL active the presence of the A aggregate in our diamonds has been indirectly inferred from the existence of the PL band A (originating from a complex consisting of an A-form nitrogen and an acceptor) in the spectra, as reported in our previous work in Ref. 33. Therefore, it may be safely assumed that, as in the type-I diamond, the A aggregate in our diamonds is the cause of most of the nitrogen-related strain.

Figures 9(a) and 9(b) show the 2.154 eV PL bands of the HF 0.2%N and the combustion films, respectively, as well as the Lorentzian and Gaussian line shape (of the same widths as the PL linewidths). It can be seen from the figures that both PL line shapes exhibit a high degree of symmetry. In this respect our PL bands are similar to the symmetric 2.154 eV PL line shape of Ia crystalline diamond.[11] The observed symmetry of our PL bands, applying Stoneham's theory

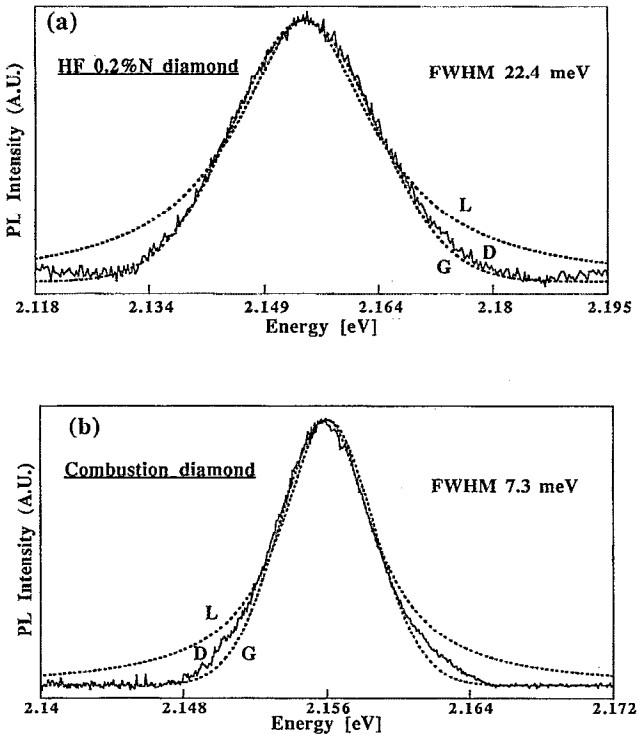

FIG. 9. The Lorentzian (L) and the Gaussian (G) fits to the 2.154 eV nitrogen PL band (D) of the (a) HF 0.2% N and (b) combustion film.

which was discussed in Sec. I, implies that the 2.154 eV optical centers as well as the defects causing the strain are uniformly distributed throughout the diamond films.

It can also be seen in Figs. 9(a) and 9(b) that the PL line shape of the HF 0.2%N film is mainly a Gaussian with a very small Lorentzian component and that the line shape of the combustion film lies between a Lorentzian and a Gaussian function. The relative linewidths of the Gaussian and Lorentzian components of each of the PL bands may be found by a deconvolution procedure and can be used to determine the respective stress contributions from line- and point-type defects. The following paragraphs outline the procedure. It has been demonstrated that the Voit profile can be approximated by a linear combination of the Gaussian and the Lorentzian functions,[48]

$$I(\omega)/I_0=(1-W_L/W_V)\exp\{-2.772[(\omega-\omega_0)/W_V]^2\}$$
$$+(W_L/W_V)(1/\{1+4[(\omega-\omega_0)/W_V]^2\}), \quad (5)$$

where W_L and W_V are the Lorentzian and the Voit linewidths, respectively (to be found). Once W_L and W_V have been determined from the curve fit of the given PL line to Eq. (5), the following relation between the Lorentzian and Gaussian linewidths,[48]

$$W_V=(W_L/2)+\sqrt{(W_L^2/4)+W_G^2}, \quad (6)$$

is used to find the Gaussian linewidth component W_G.

Figure 10 shows that the PL line of the combustion film (obtained from a high-resolution PL spectra) can be approximated well by Eq. (5); from the curve fit and Eq. (6) the values of W_L and W_G were calculated to be 2.3 and 6.0 meV,

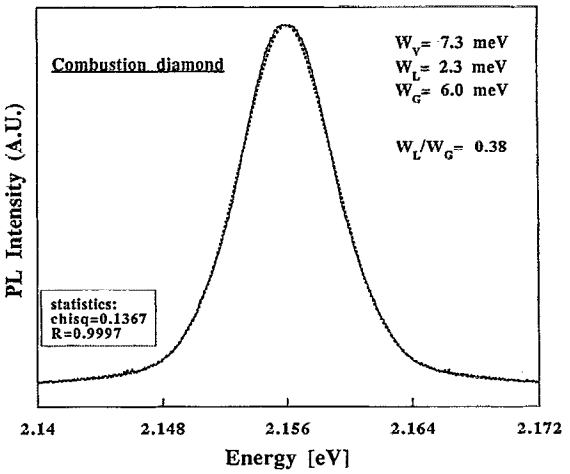

FIG. 10. The high-resolution spectra of the 2.154 eV PL band of the combustion diamond. The curve fit to the Voit profile [Eq. (5)] is presented by the dashed line. In order to get a meaningful fit, a bilateral symmetric spectra was derived by mirroring the side which exhibits the lowest background noise.

respectively. The ratio of $W_L/W_G=0.38$ implies that the Gaussian stress, which will be referred to as S_G, is approximately 2.6 times greater than the Lorentzian stress S_L. The same analytical procedure was performed on the PL band of the HF 0.2%N and its results are presented in Fig. 11. The values of W_L and W_G shown there are 3.2 and 20.8 meV, respectively; hence the Gaussian stress in this sample is ~7 times greater than the Lorentzian stress.

We next proceed to assign stress values to the observed Gaussian and Lorentzian line-broadening components. It has been demonstrated that the total internal stress $S(=S_L+S_G)$, in a given diamond sample may be obtained from the linewidth W of a nitrogen PL band via the following approximation[13,49]

$$S\cong W/10, \quad (7)$$

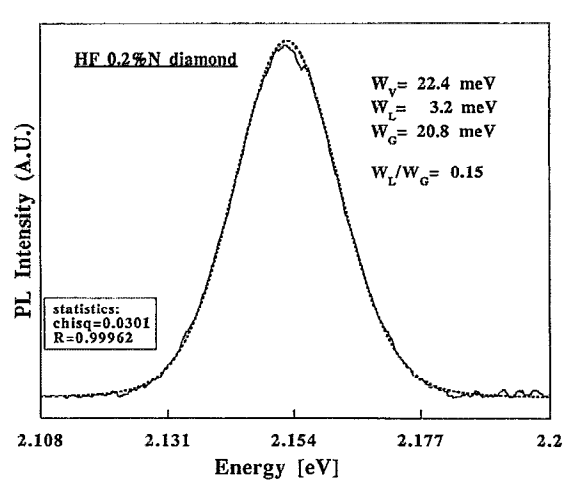

FIG. 11. The high-resolution spectra of the 2.154 eV PL band of the HF 0.2%N diamond film. The curve fit of the Voit profile [Eq. (5)] is presented by the dashed line.

TABLE IV. The linewidth of the 2.154 eV PL nitrogen bands and the Gaussian and Lorentzian stress components.

Sample	FWHM (meV)	Total stress S (GPa)	S_G (GPa)	S_L (GPa)
Combustion	7.3	0.73	0.53	0.20
HF 0.2%N	22.4	2.24	1.95	0.29

where S is in units of GPa and the linewidth W is in meV. Hence, the stress of the combustion and the HF 0.2%N samples as obtained from the PL linewidths are ~0.73 and 2.24 GPa, respectively. These stress values are of similar order of magnitude and consistent with the compressive stress values obtained previously from the Raman shift, implying that the Raman shift and the PL line broadening result from the same compressive stress sources. Combining the results calculated via Eq. (7) for the S with the previously calculated ratios W_L/W_G ($\equiv S_L/S_G$) we find that for the combustion sample the Lorentzian stress S_L ~0.20 GPa and the Gaussian stress S_G~0.53 GPa, while for the HF 0.2%N sample S_L~0.29 GPa and S_G~1.95 GPa. Table IV summarizes the above results for both samples.

According to the results listed in Table IV, we conclude that the HF 0.2%N and the combustion samples exhibit mainly a Gaussian stress and to a much smaller degree a Lorentzian stress. Therefore line-type defects contribute far more to the stress existing in the diamond thin films than the point defects.

The nitrogen A aggregates and the dislocations, since they are classified as point defects and line defects, respectively, are expected to contribute a Lorentzian and a Gaussian component, respectively, to the PL line band; however, the graphitic phase had not been definitely classified as to defect type. Here we present an analysis concerning the form the graphitic phase takes in the diamond films.

The linewidths of the 2.154 eV optical center in type Ia (~0.1–0.3 at. %N) and IIb (nominal N concentration) have been reported to be 4.45 and 1.49 meV respectively, and have been attributed to the strain imposed by the A aggregates.[11] These linewidths are comparable (up to deviation due to the N concentration and the presence of the silicon impurity) to the ones calculated for the HF 0.2%N (0.28 at. % N, W_L=3.2 meV) and combustion (0.06 at. % N, W_L=2.3 meV) samples. Hence we suggest that the Lorentzian linewidth for both samples can be attributed mainly to the A aggregate and silicon point defects with no appreciable contribution from the graphitic phase. The conclusion that the graphitic phase does not contribute to the Lorentzian linewidth implies that the graphitic is not in the form of a point defect (which would appear as a dispersed form of sp^2 bonding throughout the sample) and that the graphitic stress field is of a Gaussian form associated with dislocation type defect. Graphitization study of natural diamond has shown evidence of a two-dimensional structure of the graphitic phase in the diamond crystal.[50] Also, it has been concluded, from the atomic structure calculations of amorphous carbon that the most stable arrangement of sp^2 sites is the two-dimensional form.[51] These findings support our results because the diamond film has material characteristics similar to those of the crystal diamond and amorphous carbon.[33]

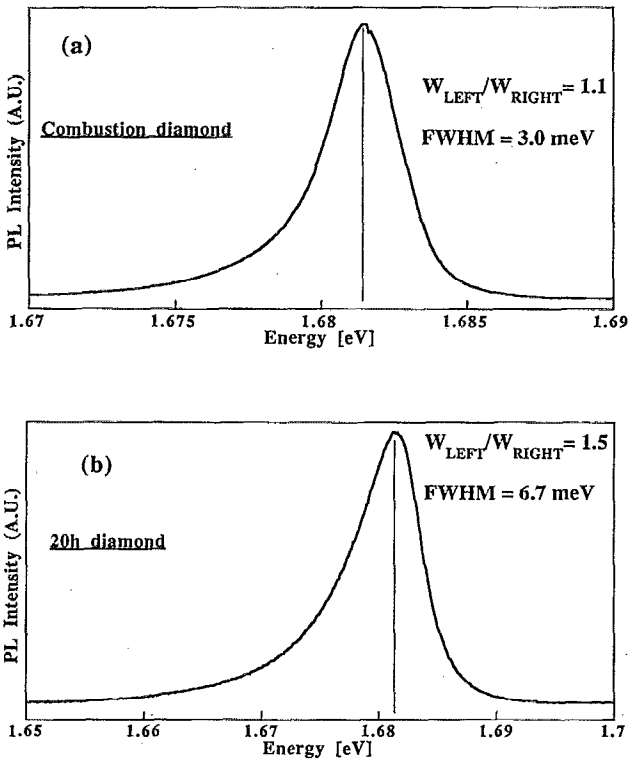

FIG. 12. The asymmetric 1.681 eV silicon PL band of the (a) combustion and (b) 20 h diamond.

Since there is no way to further deconvolute the Gaussian linewidth we cannot determine the actual contribution to the stress from the dislocations and the graphitic phase; however, based on the correlation found between the graphitic concentration and the stress (see Fig. 8) we expect the graphitic contribution to the internal compressive stress to be appreciable. In summary, we determined that the nitrogen optical centers interact mainly with the graphitic stress field, and the nitrogen centers as well as the graphitic phase are uniformly distributed throughout the film.

B. The 1.681 eV silicon optical center

The PL band at 1.681 eV is a very characteristic feature in the spectra of many diamond films grown on silicon substrate: In natural crystal diamond this PL band appears only after silicon implantation; hence, the 1.681 eV band has been attributed to an optical center containing at least one silicon atom.[25,30] No definite model of the structure and symmetry of this center has yet been formulated. The structure has been suggested, however, to consist of two interstitial silicon atoms or of a silicon atom and a vacancy.[30,52]

In this subsection an investigation concerning the spatial distribution and the structure of the 1.681 eV PL band is presented. Figures 12(a) and 12(b) present the high-resolution PL spectra of the silicon center obtained from the combustion and 20 h samples, respectively. It can be seen in the figures that the PL bands exhibit very strong line asymmetry.

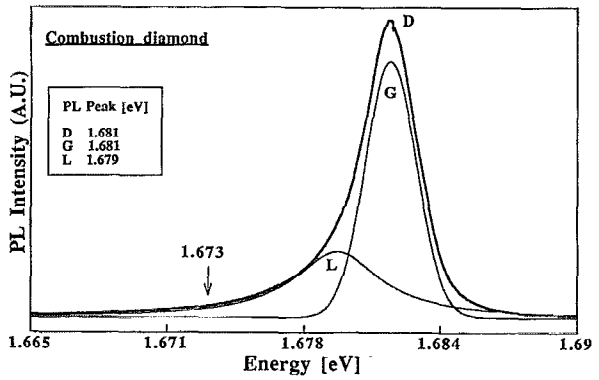

FIG. 13. The deconvolution of the silicon PL band (D) into the two underlying components: the Gaussian (G) and the Lorentzian (L). The neutral vacancy band at 1.673 is not present as one of the underlying components.

One possible mechanism that might affect the symmetry of a PL line shape is the existence of an underlying PL band (due to a different optical center which luminesces in the same energy range). Such an underlying PL band in the energy range of the 1.681 eV might be the PL band at 1.673 eV due to the GR1 optical center which consists of a neutral vacancy.[53] The GR1 optical center is a very common center occurring in natural diamond; however, no such center has ever been observed in diamond films. In order to check the possibility that the GR1 PL band might be the cause of the observed line asymmetry, we deconvoluted the 1.681 eV line into its possible line combinations. The best fit of our data to a combination of an underlying and a main band yielded an underlying band which did not match the GR1 PL peak position, as can be seen in Fig. 13; hence, we can exclude the above mechanism as being responsible for the observed line asymmetry.

A more plausible mechanism which may explain the strong PL line asymmetry of the silicon center is the strong correlation of the optical centers with the surrounding defects. In our previous work it was found that the silicon centers are incorporated into the diamond matrix during the initial stages of growth, and thus reside mainly at the silicon/diamond interface.[32] Such two-dimensional distribution of the optical centers would be expected to affect the symmetry of the PL line shape since the optical centers are subjected to the interfacial stress more than to the stress distributed throughout the film. An exact analysis concerning the 1.681 eV PL band asymmetry may be concluded in a future investigation. At present we may suggest with reasonable certainty, however, that the nonuniform concentration of the silicon optical centers in the diamond films is the cause of the asymmetric PL band.

It was observed that the silicon PL linewidths are significantly narrower than the nitrogen PL linewidths (see Figs. 9 and 12) for which we offer the following explanations. The PL linewidth depends on the concentration and the strength of the strain sources in a given film as well as on the structure of the optical center itself.[9,12] Since a soft optical center would comply to the stress more readily than a rigid optical center, when the two optical center types exist in the same film and are thus subjected to a similar internal stress any difference in the PL linewidths must reflect differences in their structures. Our combustion diamond sample contains both the 1.681 and the 2.154 eV optical centers: the linewidth of the 2.154 eV PL band is 7.3 meV and that of the 1.681 eV band is 3.0 meV. The difference in the linewidths may imply that the 1.681 eV center is a more rigid center than the 2.154 eV center. A possible way to explain the above observation is that the 1.681 eV center does not contain any vacancy or contains fewer vacancies than the 2.154 eV center.

A second mechanism (which may act simultaneously with the one discussed above) that may explain the narrower silicon linewidth arises from the distribution of the silicon centers next to the silicon substrate. The symmetric line shape of the nitrogen PL band implies that the nitrogen and the principal strain source, which was suggested to be the graphitic phase, are uniformly distributed in the film. The silicon optical centers, on the other hand, were concluded to reside next to the substrate; hence, types of stress other than due to interaction with the graphitic phase, such as interfacial stress, may be more crucial in the interaction. The interfacial stress which the silicon optical centers might be subjected to could arise from the thermal stress, misfit dislocation, and from some form of silicon impurity aggregations. Since the silicon PL linewidth is narrower than the nitrogen linewidth it follows that the interfacial stress is of smaller magnitude than the stress acting on the nitrogen centers. A future study will address the formulation of the line asymmetry and identification of the dominant stress source in the broadening of the silicon PL band. At present we suggest that the silicon optical center is of a rigid structure and is subjected to an interfacial stress of a lesser magnitude than the stress than exists throughout the diamond film.

V. CONCLUSIONS

Photoluminescence and Raman spectroscopy were employed to investigate the stress state and stress sources in the diamond thin films as well as to determine the defects types and their distributions in the films.

Our analysis indicates that the thin diamond samples exhibit internal stress which is compressive. The magnitude of the thermal stress due to the difference in the thermal expansion of the diamond and silicon is insignificant relative to the magnitude of the internal compressive stress in the films. From the correlation of the Raman linewidth (which was established to broaden via impurity scattering) to the internal stress and from the symmetric Lorentzian Raman line shape, we conclude that the various defects and impurities in the films are the sources of the compressive internal stress. The impurities and defects in the diamond films which were identified are the nitrogen and silicon point defect complexes, the graphitic phase of the disordered sp^2 bonding, and line defects such as dislocations.

The relative concentration of the graphitic phase in the diamond films correlates well with the internal stress. The small deviation in this correlation is due to the compressive stress contributions from the various other impurities present in the diamond films; hence, we conclude that the graphitic phase introduces stress in the diamond matrix that is com-

pressive in nature. We also hypothesize that the graphitic phase is the major stress source contributor and that its structural form is not of a point defect, that is, it is not in the dispersed form of sp^2 bonding. These conclusions follow from

(a) the established correlation of the graphitic concentration to the internal stress and
(b) the attribution of the Lorentzian stress to the nitrogen and silicon point defects and the dominance of the Gaussian stress.

The observed PL line-shape symmetry of the 2.154 eV nitrogen-vacancy center indicates that the stress sources that the optical centers interact with as well as the 2.154 eV optical centers are uniformly distributed throughout the diamond film. On the other hand, the strong asymmetry of the 1.681 eV PL band indicates that the 1.681 eV optical centers do not form a uniform distribution. This conclusion is supported by the previous finding about the biased incorporation of the centers into the diamond film during the initial stages of growth. A comparison of the linewidths of the 1.681 and 2.154 eV PL bands leads to the conclusion that the 1.681 eV optical center may be a more rigid center than the 2.154 eV center and that both optical centers interact with different stress sources.

ACKNOWLEDGMENTS

The authors gratefully acknowledge the collaboration and support of Peter Mills from the Computer Science Department at Duke University. We also wish to thank J. T. Glass for his constructive criticism and suggestions. Thanks are also extended to Kevin Turner from NRL and Phillip Morrison for supplying the diamond film samples and Terri McCormick for many helpful discussions. This work was supported in part by the ONR through contracts No. N00014-93-J-0437 and No. N00014-92-J-1477.

[1] M. H. Grimsditch, E. Anastassakis, and M. Cardona, Phys. Rev. B **18**, 901 (1978).
[2] S. K. Sharma, H. K. Mao, P. M. Bell, and J. A. Xu, J. Raman Spectrosc. **16**, 350 (1985).
[3] S. A. Lyon, R. J. Nemanich, N. M. Johnson, and D. K. Biegelsen, Appl. Phys. Lett. **40**, 316 (1981).
[4] W. J. Meng and T. A. Perry, J. Appl. Phys. **76**, 7824 (1994).
[5] S. S. Mitra, O. Brafman, W. B. Daniels, and R. K. Crawford, Phys. Rev. **186**, 942 (1969).
[6] M. Cardona, Proc. SPIE **822**, 2 (1987).
[7] E. Anastassakis, A. Pinczuk, E. Burstein, F. H. Pollak, and M. Cardona, Solid State Commun. **8**, 133 (1970).
[8] M. Yoshikawa, G. Katagiri, H. Ishida, A. Ishitani, M. Ono, and K. Matsumura, Appl. Phys. Lett. **55**, 2608 (1989).
[9] A. M. Stoneham, Rev. Mod. Phys. **41**, 82 (1969).
[10] A. M. Stoneham, Proc. Phys. Soc. **89**, 909 (1966).
[11] G. Davies, J. Phys. C **3**, 2474 (1970).
[12] A. E. Hughes, J. Phys. Chem. Solids **29**, 1461 (1968).
[13] T. Evans, S. T. Davey, and S. H. Robertson, J. Mater. Sci. **19**, 2405 (1984).
[14] Y. H. Lee, K. J. Bachmann, J. T. Glass, Y. M. LeGrice, and R. J. Nemanich, Appl. Phys. Lett. **57**, 1916 (1990).
[15] H. Windischmann, G. F. Epps, Y. Cong, and R. W. Collins, J. Appl. Phys. **69**, 2231 (1991).
[16] F. A. Doljack and R. W. Hoffman, Thin Solid Films **12**, 71 (1972).
[17] W. J. Borer, S. S. Mitra, and K. V. Namjoshi, Solid State Commun. **9**, 1377 (1971).
[18] R. J. Nemanich, S. A. Solin, and R. M. Martin, Phys. Rev. B **23**, 6348 (1981).
[19] I. H. Campbell and P. M. Fauchet, Solid State Commun. **58**, 739 (1986).
[20] J. W. Ager, D. K. Veirs, and G. M. Rosenblatt, Phys. Rev. B **43**, 6491 (1991).
[21] B. DiBartolo, in *Optical Interactions in Solids* (Wiley, New York, 1969).
[22] A. T. Collins and S. C. Lawson, J. Phys. Condens. Matter **1**, 6929 (1989).
[23] A. T. Collins, M. Kamo, and Y. Sato, J. Mater. Res. **5**, 2507 (1990).
[24] G. Davies, J. Phys. C **12**, 2551 (1979).
[25] J. Ruan, W. J. Choyke, and W. D. Partlow, J. Appl. Phys. **69**, 6632 (1991).
[26] J. A. Freitas, J. E. Butler, and U. Strom, J. Mater. Res. **5**, 2502 (1990).
[27] T. Feng and B. D. Schwartz, J. Appl. Phys. **73**, 1415 (1993).
[28] R. J. Graham, T. D. Moustakas, and M. M. Disko, J. Appl. Phys. **69**, 3212 (1991).
[29] R. J. Graham and K. V. Ravi, Appl. Phys. Lett. **60**, 1310 (1992).
[30] V. S. Vavilov, A. A. Gippius, A. M. Zaitsev, B. V. Deryagin, B. V. Spitsyn, and A. E. Aleksenko, Sov. Phys. Semicond. **14**, 1078 (1980).
[31] L. H. Robins, L. P. Cook, E. N. Farabaugh, and A. Feldman, Phys. Rev. B **39**, 13 367 (1989).
[32] L. Bergman, B. R. Stoner, K. F. Turner, J. T. Glass, and R. J. Nemanich, J. Appl. Phys. **73**, 3951 (1993).
[33] L. Bergman, M. T. McClure, J. T. Glass, and R. J. Nemanich, J. Appl. Phys. **76**, 3020 (1994).
[34] R. J. Graham, Mater. Res. Soc. Symp. Proc. **242**, 97 (1992).
[35] B. E. William, J. T. Glass, R. F. Davis, K. Kobashi, and T. Horiuchi, J. Vac. Sci. Technol. A **6**, 1819 (1988).
[36] W. Zhu, A. R. Badzian, and R. Messier, J. Mater. Res. **4**, 659 (1989).
[37] R. E. Shroder, R. J. Nemanich, and J. T. Glass, Phys. Rev. B **41**, 3738 (1990).
[38] L. H. Robins, E. N. Farabaugh, and A. Feldman, J. Mater. Res. **5**, 2456 (1990).
[39] A. R. Badzian, T. Badzian, R. Roy, R. Messier, and K. E. Spear, Mater. Res. Bull. **23**, 531 (1988).
[40] A. Somashekhar, S. P. Bozeman, J. T. Glass, P. W. Morrison, and J. T. Prater, in *Advances in New Diamond Science and Technology* (MYU, Tokyo, 1994), p. 225.
[41] L. I. Maissel and R. Glang, in *Handbook of Thin Film Technology* (McGraw–Hill, New York, 1970).
[42] J. A. Baglio, B. C. Farnsworth, S. Hankin, G. Hamill, and D. O'Neil, Thin Solid Films **212**, 180 (1992).
[43] Y. M. LeGrice, master thesis, North Carolina State University, 1990.
[44] B. R. Stoner, Ph.D thesis, North Carolina State University, 1992.
[45] A. M. Zaitsev, A. A. Gippius, and V. S. Vavilov, Sov. Phys. Semicond. **16**, 252 (1982).
[46] Gordon Davies, J. Phys. C **9**, L537 (1976).
[47] Gordon Davies, Nature **228**, 758 (1970).
[48] E. E. Whiting, J. Quantum Spectrosc. Radiat. Transfer **8**, 1379 (1968).
[49] A. T. Collins and H. Robertson, J. Mater. Sci. Lett. **4**, 681 (1985).
[50] T. Evans, in *The Properties of Diamond*, edited by J. E. Field (Academic, London, 1979), p. 403.
[51] J. Robertson and E. P. O'Reilly, Phys. Rev. B **35**, 2946 (1987).
[52] G. Davies, in *The Properties and Growth of Diamond*, edited by G. Davies (INSPEC, The Institute of Electrical Engineers, London, 1994), p. 133.
[53] G. Davies, in *Chemistry and Physics of Carbon*, edited by P. L. Walker (Marel Dekker, New York, 1977), Vol. 13, p. 1.